International Journal of Pharmaceutics 595 (2021) 120274

Contents lists available at ScienceDirect

International Journal of Pharmaceutics

journal homepage: www.elsevier.com/locate/ijpharm

Modulation of the powder properties of lamotrigine by crystal forms

Oisín N. Kavanagh [a,*], Chenguang Wang [b], Gavin M. Walker [a], Changquan Calvin Sun [b,*]

[a] Synthesis and Solid State Pharmaceutical Centre (SSPC), The SFI Research Centre for Pharmaceuticals, Department of Chemical Sciences, Bernal Institute, University of Limerick, Limerick, Ireland

[b] Pharmaceutical Materials Science and Engineering Laboratory, Department of Pharmaceutics, College of Pharmacy, University of Minnesota, 9-127B Weaver-Densford Hall, 308 Harvard Street S.E., Minneapolis, MN 55455, USA

ARTICLE INFO

Keywords:
Solid form optimisation
Cocrystal
Crystal engineering
Tableting
Direct compaction
Multidrug
High drug load

ABSTRACT

The mechanical properties of powders determine the ease of manufacture and ultimately the quality of the oral solid dosage forms. Although poor mechanical properties of an active pharmaceutical ingredient (API) can be mitigated by using suitable excipients in a formulation, the effectiveness of that approach is limited for high dose drugs or multidrug tablets. In this context, improving the mechanical properties of the APIs through solid form optimisation is a good strategy to address such a challenge. This work explores the powder and tableting properties of various lamotrigine (LAM) solid forms with the aim to facilitate direct compression by overcoming the poor tabletability of LAM. The two drug-drug crystals of LAM with nicotinamide and valproic acid demonstrate superior flowability and tabletability over LAM. The improved powder properties are rationalised by structure analysis using energy framework, scanning electron microscopy, and Heckel analysis.

1. Introduction

Since the first pharmaceutical tablet was produced in England in 1844, the physics relating to the transformation of powdered pharmaceuticals into compacts has become of increasing importance to researchers in pharmaceutical science (Kebler, 1914). The latest desire to develop directly compressible powder formulations (Bolhuis and Armstrong, 2006; Schaller et al., 2019) draws interesting parallels to the times when direct compression (DC) was the only option. The renewed interest in DC is partially driven by its prominent role in the continuous manufacturing (CM) process, which is been intensely explored by the pharmaceutical industry as it moves away from traditional batch processes for better quality, efficiency, and agility of manufacturing afforded by the CM (Lee et al., 2015; Mascia et al., 2013; Poechlauer et al., 2012). CM is particularly important for green chemistry to achieve the significantly improved efficiency of the processes by reducing the number of processing steps (Li and Trost, 2008).

Naturally, active pharmaceutical ingredients (APIs) do not always exhibit desired pharmaceutical properties, such as tabletability, compressibility, and flowability. Therefore, they need to be appropriately formulated to enable successful tablet manufacturing. For a given powder or a powder blend, powder flow properties are often defined by particle size, shape and surface chemistry (Hou and Sun, 2008). Whereas compressibility can be described by a number of mathematical models, with the Heckel analysis being the most utilised to describe plastic deformation (Heckel, 1961; Paul and Sun, 2017a). Tabletability is the ability of a material to form a compact with a certain tensile strength across a range of compaction pressures (Joiris et al., 1998; Sun and Grant, 2001b). These properties are often achieved by blending an API with suitable excipients to overcome any deficient powder properties. However, for a number of challenging drugs, such as canagliflozin (Schaller et al., 2019) and ibuprofen (Han et al., 2013), the utility of excipients and design methodologies are pushed to their limits in the quest for a single dosage system.

For high-API load tablets, including many multidrug systems (Kavanagh et al., 2018), and high dose drugs (e.g., metformin or paracetamol, up to 1 g per dose), the use of excipients to overcome difficulties arising from deficient powder properties of APIs is limited because the overall size of the tablet cannot be too large to swallow (Dave et al., 2015). In these cases, generating solid forms with enhanced powder properties to reduce the quantity of excipients in formulations required for successful tablet manufacturing is of value (Kavanagh et al., 2019a).

Much of the published literature on mechanical properties of different solid forms compares a pair of solid forms (e.g., cocrystals, solvates, and salts) in a single paper (Ainurofiq et al., 2018; Hiendrawan

* Corresponding authors.
E-mail addresses: Oisin.Kavanagh@ul.ie (O.N. Kavanagh), sunx0053@umn.edu (C.C. Sun).

https://doi.org/10.1016/j.ijpharm.2021.120274
Received 4 December 2020; Received in revised form 31 December 2020; Accepted 8 January 2021
Available online 21 January 2021

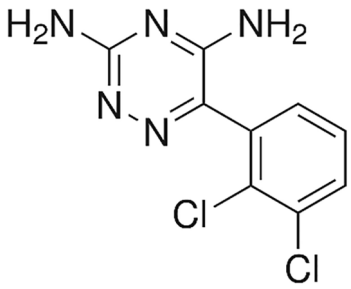

Scheme 1. Molecular structure of lamotrigine.

et al., 2016; Joshi et al., 2018; Karki et al., 2009; Suihko et al., 2001; Wang et al., 2017). This has led to useful information but gaining comprehensive understanding of the crystal structure–mechanical property relationships would benefit from simultaneous investigation of several crystal forms in a single study, which is beginning to emerge in the literature (Sanphui et al., 2015; Yadav et al., 2020). We synthesised several solid forms of lamotrigine (LAM, Scheme 1) with a variety of structures to probe the effect of crystal packing on the mechanical characteristics (Fig. 1). These include lamotrigine-acetic acid (LAMAA), lamotrigine-isopropanol (LAMIPA), and lamotrigine-chloride (LAMCL) in addition to two drug-drug complexes, lamotrigine-nicotinamide hydrate (LAMNIC) and lamotrigine-valproic acid (LAMVAL) (Kavanagh et al., 2019b).

2. Materials and methods

Lamotrigine was purchased from Baoji Guokang Bio-Technology Co. Ltd. and used without further purification. All other solvents and reagents were purchased from Sigma-Aldrich and used as received.

2.1. Synthesis of solid forms

All solid forms were synthesised by following published methods. Phase purity of each powder was confirmed by PXRD. The powders were sieved and only the 100–180 μm size fractions were further characterised because such a size range is typical of drugs for direct compaction (Shekunov et al., 2007).

Lamotrigine chloride salt. 8 g Lamotrigine was added to a solution containing 100 mL 10 M HCl and stirred at 500 rpm for 48 h. The product was recovered by vacuum filtration, washed with ice cold water and then dried in air.

Lamotrigine/valproic acid (1:2) ionic cocrystal. 8 g lamotrigine was added to a 100 mL solution containing excess valproic acid (10 mL) and stirred at 500 rpm for 48 h. The product was recovered by vacuum filtration, washed with ice cold water and then dried in air.

Lamotrigine/acetic acid (1:2) ionic cocrystal. 8 g lamotrigine was added to 100 mL acetic acid and stirred at 500 rpm for 48 h. The product was recovered by vacuum filtration, washed with ice cold water and then dried in air.

Lamotrigine/isopropyl alcohol (IPA) solvate. 8 g lamotrigine was added to 100 mL IPA and stirred at 500 rpm for 48 h. The product was recovered by vacuum filtration and then dried in air.

Lamotrigine/nicotinamide (1:1) cocrystal hydrate. Lamotrigine (to 0.5 M) was added to a 100 mL water containing 3.5 M nicotinamide in 2% w/w sodium lauryl sulphate and stirred at 500 rpm for 48 h. The product was recovered by vacuum filtration, washed with ice cold water and then dried in air.

2.2. Powder characterisation

Powder true density was determined for each solid form using a helium pycnometer (AccuPyc II 1340 Micrometrics Instrument Corp, UK), sample density was determined after 10 cycles. Powder rheology was determined using an FT4 powder rheometer (Freeman Technology, Tewkesbury, UK). Compressibility is defined as the percentage volume change under a specified compression pressure up to 15 kPa. Powder permeability determines the ease of air to pass through the powder bed whilst it is compressed under a 15 kPa pressure, which is described by a modified Darcy's law (Cordts and Steckel, 2012). Powders are preconditioned with a helical blade prior to testing to ensure repeatability.

Raman spectra of the powders and tablet immediately after compaction were collected using a Raman spectrometer (LabRAM HR Evolution, Horiba, UK) with a 514 nm excitation laser, 350–1650 cm^{-1} scan range, and 4 cm^{-1} resolution using a 50 × objective lens with 60 s exposure time, 50% laser power, and 4 accumulated scans per spectrum.

X-ray powder diffraction (XRPD) patterns were collected in Bragg–Brentano geometry on a PANalytical Empyrean diffractometer equipped with a sealed tube (Cu Kα12, λ = 1.5418 Å) an 1D X'Celerator detector between 4 and 40° 2θ. Variable temperature PXRD data were collected in Bragg–Brentano geometry on a X'Pert MPD Pro equipped with an Anton-Paar TK450 stage, a sealed tube (Cu Kα12, λ = 1.5418 Å) and a 1D X'Celerator detector in the 4–30° (2θ) range.

Microphotographs of each sample were collected after placing it onto a carbon tape and then sputter coated with gold–palladium for 90 s with a 20 mA current. Samples were then scanned at 2.5 kV with 16 mm working distance using a high-resolution field-emission electron microscope (SEM, Hitachi SU-70, Hitachi, Japan).

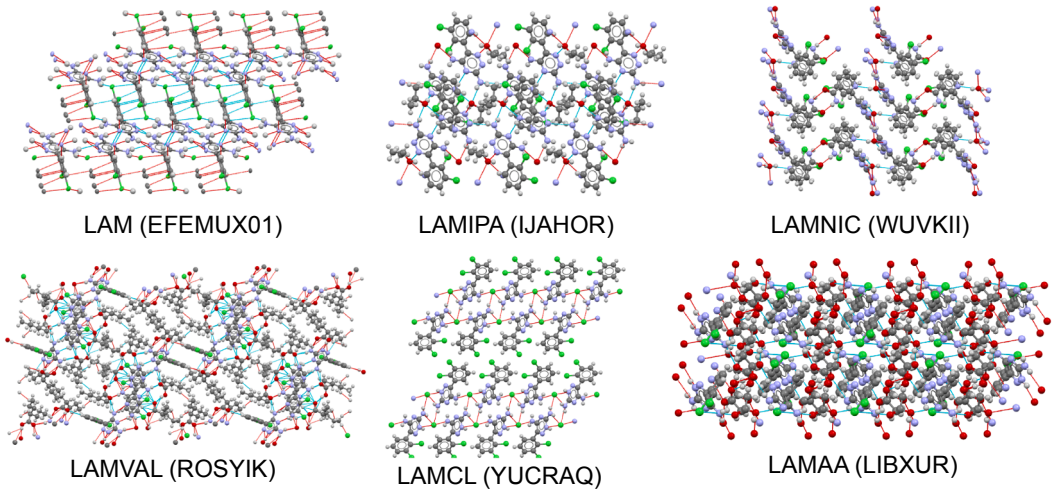

Fig. 1. Structures of six LAM solid forms (CSD refcodes are in parentheses).

2.3. Tablet preparation

A single punch press (Gamlen Instruments, UK) equipped with a GTP-500-010 load cell was used to generate flat, cylindrical tablets of 6 mm diameter with an average thickness of 3 mm. Approximately 105 mg of sample was weighed on an analytical balance and transferred to die manually to generate a ~100 mg tablet (due to loss of powder on transfer). Compacts were made with one-sided compression and no pre-compression at pressures of 35, 70, 105, 140, and 175 MPa without holding at the peak pressure. Punch speed was 1 mm/s. Compaction data was collected at a sampling rate of 200 data points per second. Tablets were then stored in sealed polyethylene bags for 24 h to enable stress relaxation. All compacts were made with the same compaction parameters. Ejection data was collected at maximum pressure (175 MPa) at the same punch speed and sampling rate. Each tablet was prepared in triplicate.

2.4. Tablet characterisation

Tablet dimensions were measured using a digital calliper and diametrical breaking strength of the tablet was conducted on a hardness tester (PTB 311E, Pharma Test, Germany)

Tablet porosity was calculated according to Eq. (1):

$$Tablet\ \ porosity = 1 - \frac{Tablet\ \ Density}{True\ \ Powder\ \ Density} \quad (1)$$

Tensile strength was calculated using Eq. (2):

$$Tensile\ \ strength = \frac{2 \times (Breaking\ \ strength)}{\pi \times (Diameter) \times (Thickness)} \quad (2)$$

Elastic recovery (%) was calculated at 175 MPa according to Eq. (3):

$$Elastic\ \ recovery = \frac{h - h_{pressure}}{h_{pressure}} \times 100 \quad (3)$$

where $h_{pressure}$ is the powder bed height at maximum pressure and h is the thickness of the tablet after compaction at constant diameter (6 mm).

2.5. Heckel analysis

The in-die tablet porosity - pressure data was analysed using Eq. (4) (Heckel, 1961; Sun and Grant, 2001a):

$$-ln(1 - tablet\ \ porosity) = KP + A \quad (4)$$

where P is the compaction pressure, K is the slope of the linear portion of the Heckel plot and A is the y-axis intercept. The mean yield pressure, $P_y = 1/K$, was calculated to assess plasticity of the powders.

2.6. Computational structure analysis

The crystal morphology and attachment energy were calculated using the Morphology module in the Materials Studio 8.0. (Biovia Software Inc., San Diego, CA, USA). Calculations were carried out using the following parameters: Compass force field with associated charges at fine quality (Li et al., 2017), the "Ewald" electrostatic summation method, "atom based" van der Waals summation, and a minimum d_{hkl} of 0.8 Å.

The pairwise intermolecular interaction energy was estimated using CrystalExplorer (Turner et al., 2017) and Gaussian09 (Frisch et al., 2009) with experimental crystal geometry. Considering the uncertainty of hydrogen position by single crystal X-ray diffraction, the hydrogen positions were normalised to standard neutron diffraction values during the calculation. The total intermolecular interaction energy for a given pair of molecules, is calculated using the CE-B3LYP electron densities model consisting of the electrostatic, polarisation, dispersion, and exchange-repulsion components, with scale factors of 1.057, 0.740, 0.871, and 0.618, respectively, (Turner et al., 2014). The intermolecular interactions between molecules with separation distance more than 3.8 Å are ignored. The intermolecular interaction energies are represented by cylinders connecting the centres of mass of molecules with the cylinder thickness proportional to the interaction energy (Turner et al., 2015).

The quantitative layer topology analysis in crystals was obtained using CSD Python program (Bryant et al., 2018). This geometric analysis approach identified the most likely slip plane based on the lowest degree of interpenetration and highest distance between the separated molecular layers.

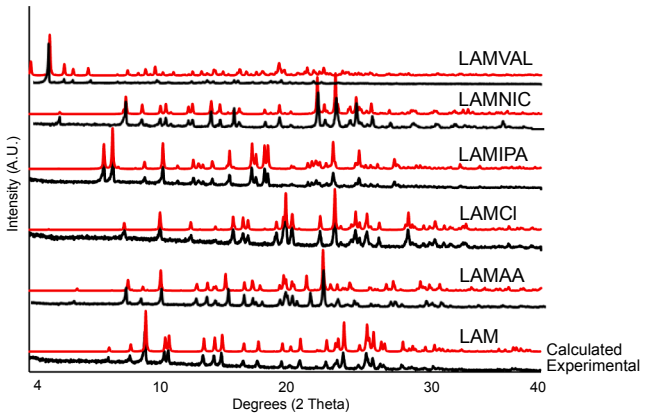

Fig. 2. Powder XRD diffractograms of six lamotrigine solid forms in comparison to patterns calculated from crystal structures deposited in the Cambridge Structural Database.

Table 1
Summary of solid form characteristics.

Solid form	CSD code	True density (g/cm^3) (n = 10) (mean ± SE)	P_y (MPa) (n = 3) (mean ± SE)	In-die elastic recovery (n = 3) (mean ± SE)
LAM	EFEMUX01	1.5612 ± 0.0007	66.5 ± 7.0	5.65 ± 0.14
LAMVAL	ROSYIK	1.2431 ± 0.0010	54.3 ± 3.8	10.28 ± 0.09
LAMAA	LIBXUR	1.4434 ± 0.0013	81.9 ± 15	6.28 ± 0.19
LAMIPA	IJAHOR	1.5193 ± 0.0009	117.2 ± 1.6	5.20 ± 0.25
LAMNIC	WUVKII	1.5016 ± 0.0010	142.6 ± 37.3	5.89 ± 0.23
LAMCL	YUCRAQ	1.6399 ± 0.0022	68.3 ± 3.2	8.95 ± 0.34

3. Results and discussion

All powders were phase pure based on their PXRD patterns (Fig. 2). Table 1 summarises their P_y and true densities.

Different mechanical properties of powders are expected to affect the choice of the most suitable solid form for use in a tablet formulation. Key characteristics of drugs, such as tabletability, compressibility and flowability, must be determined to understand how a powder will perform during the manufacturing processes to assure the quality of tablets. These properties are often affected by the shape and size of the particles (Sun and Grant, 2001b). For pure drug powders, the shape and size of crystals or crystal agglomerates can largely explain their different flowability (Fu et al., 2012; Ridgway and Rupp, 1969).

As the same narrow sieve fractions of all of the powders were used, we focused on the particle morphology to explain their different flowabilities. Based on the SEM micrographs (Fig. 3), the powders of the 6 solid forms can be classified into three morphological groups, 1) smooth, round crystals (LAMNIC, LAMIPA and LAMAA), 2) large agglomerates of small crystals (LAM and LAMCL), and 3) elongated agglomerates

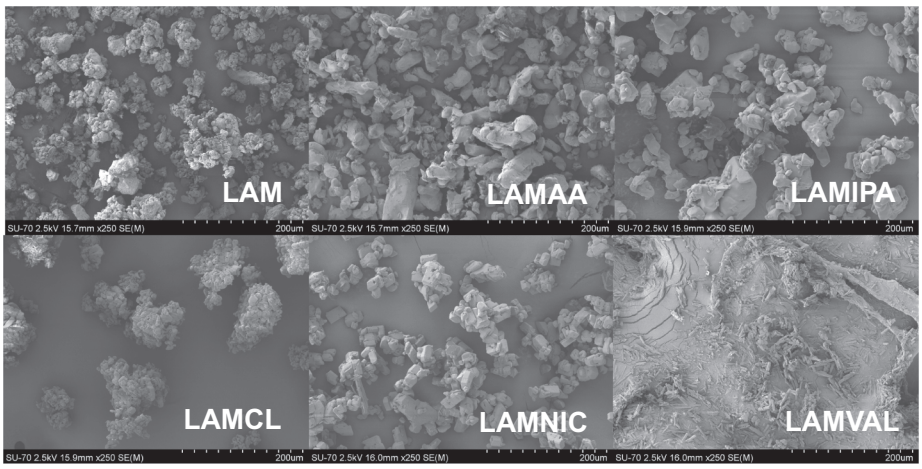

Fig. 3. Scanning Electron Microscopy (SEM) images of solid forms of LAM (250x magnification, scale 200 μm).

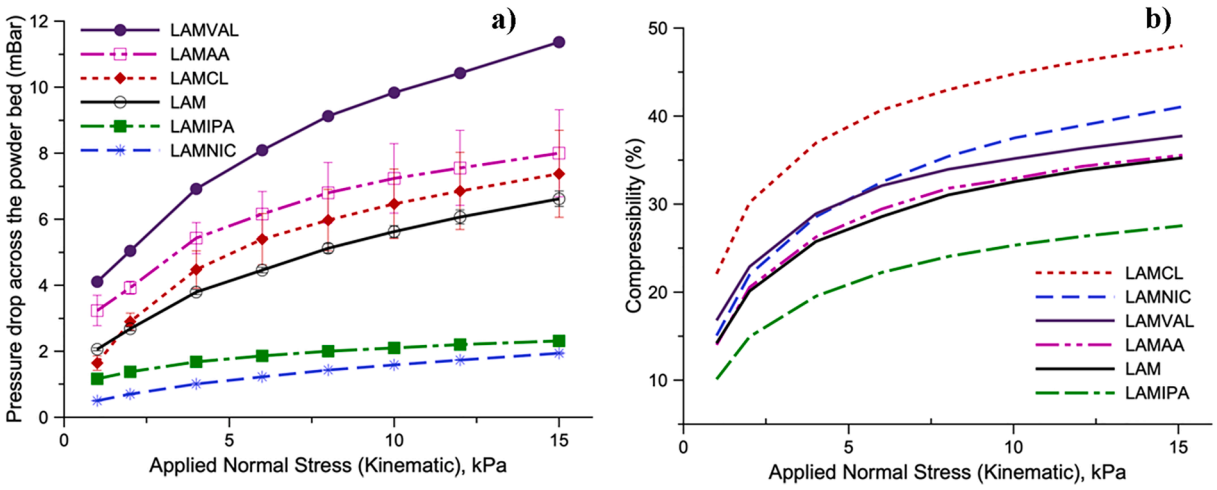

Fig. 4. Flowability of six LAM powders (a) permeability and (b) compressibility.

consisting of fine needles (LAMVAL). Agglomeration leads to powder properties distinct from the primary crystals, which can effect flowability, densification processes during tableting, and the tabletability (Bika et al., 2001).

Before a pharmaceutical solid is compacted it must flow through various hoppers and pipes to reach the tablet press. Therefore, it is useful to determine powder rheology of the various LAM solid forms (Fig. 4).

Poor powder permeability can lead to capping or lamination of tablets alongside difficulties with dosage uniformity (Prescott and Barnum, 2000). The powder permeability follows the descending order of LAMNIC > LAMIPA > LAM = LAMCL = LAMAA > LAMVAL (Fig. 4a). This rank order can be rationalised from the SEM images, which identified three predominant macroscopic shapes (Fig. 3): 1) the large smooth LAMNIC and LAMIPA crystals tend to create less tortuous voids within the powder bed to enable easy air permeation, 2) the rougher shaped agglomerates of LAM and LAMCL and 3) the needle shaped morphology of LAMVAL lead to interlocked particles packing, which reduces the air permeability of these powders.

Compressibility is another parameter that correlates with flow properties. Among the 6 powders, compressibility follows the descending order of LAMCL > LAMNIC > LAM = LAMAA = LAMVAL > LAMIPA (Fig. 4b). According to the European Pharmacopeia monograph on powder flow, the measured compressibility suggests that the flow of LAMCL is “very, very poor”, those of LAM, LAMAA, LAMVAL and LAMNIC are “very poor”, and that of LAMIPA is “poor” (although it is very close to “passable”). As such, all of the powders could be described as unsuitable for further development and addition of excipients would be required to improve their powder properties (Council of Europe, 2019). Although beyond the scope of this study, the use of magnesium stearate (York, 1975) or colloidal silica (Tran et al., 2019; Zhou et al., 2013) could be used to improve their flow characteristics. However, the use of magnesium stearate for flow enhancement needs to be balanced to avoid any excessive detrimental effects on tablet strength (Strickland et al., 1956).

For particles of comparable sizes, those with smoother surfaces and more spherical shapes are generally expected to exhibit better flow properties than needle-like materials (Beck et al., 2010; Ridgway and Rupp, 1969). However, the compressibility of LAMVAL lies in the middle of the group, while that of LAMCL is the highest. This observation is inconsistent with the large and relatively round agglomerates of LAMVAL than LAMCL. A possible explanation is that these agglomerates are loosely packed, and they break into fine crystals under stress during the compressibility test. These observations highlight the fact that accurate prediction of powder properties from particle properties remains a challenge in the powder technology field. In general, reliable powder properties still need to be experimentally determined, due to the wide variety of confounding factors (Chen et al., 2020; Krantz et al., 2009).

The goal of powder compression is to obtain a tablet that is strong enough to withstand stresses during manufacturing, distribution, and storage, while also allowing tablets to fragment and disintegrate *in vivo*.

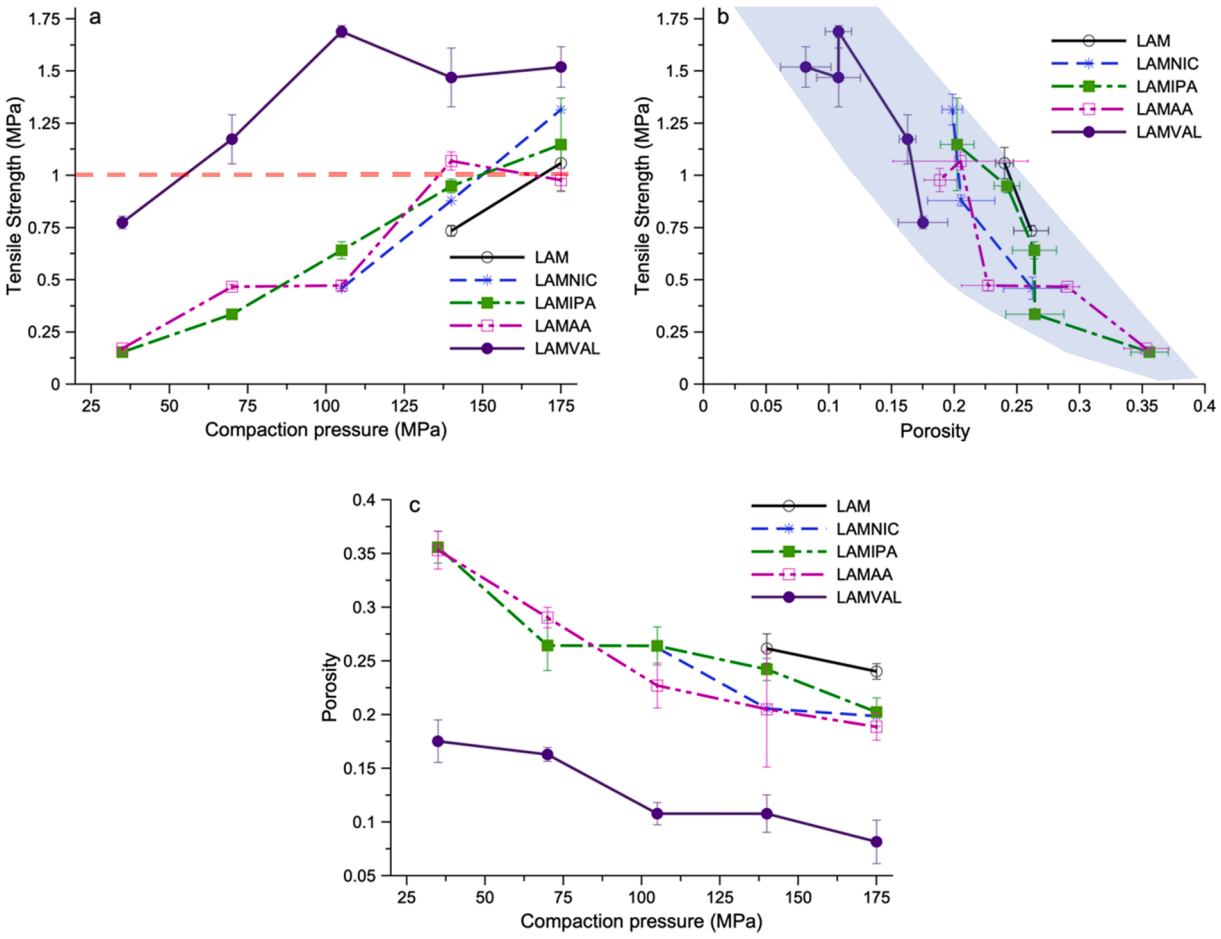

Fig. 5. Compression properties of the six LAM solid forms. a) Tabletability b) Compactibility, and c) Compressibility.

In general, 0.15 porosity is commonly the aim for compacted pharmaceuticals with an acceptable tensile strength of 1.5 MPa, as previously discussed (Podczeck, 2013, 2012; Sonnergaard, 2013). As such, the tabletability, compressibility, and compactibility of the solid forms were analysed.

Only LAMVAL, LAMIPA and LAMAA could form intact tablets over the entire range of compaction pressures tested (Fig. 5a). LAMNIC and LAM could not form intact tablet below 70 MPa and 140 MPa, respectively. Except for LAMCL, all lamotrigine solids can form tablets with a tensile strength greater than 1 MPa (Fig. 5a). When normalised by tablet porosity, tensile strength appears to fall in a common zone (Fig. 5b). Among the five crystals with intact tablets available, LAMVAL is the most compressible, yielding tablets with the lowest porosity at any given pressure (Fig. 5c). Based on limited tablet porosity data, the compressibility of LAM appears to be the worst (highest porosities), while the compressibilities of LAMIPA, LAMNIC, and LAMAA lie in between and cannot be well separated from each other due to the large variations in data (Fig. 5c). Within the precision of measured data, the comparable compactibility among the five crystals suggests comparable bonding strength. Since the bonding strengths do not significantly differ, the different tabletabilities is a result of different bonding area according to the bonding area – bonding strength interplay model for tablet tensile strength (Osei-Yeboah et al., 2016). This is supported by the correspondence between the highest tabletability and best compressibility for LAMVAL as well as the lowest tabletability and poorest compressibility for LAM (Fig. 5a,c). Following this trend, the inability of LAMCL to form intact tablets at any of the pressures tested may be attributed to its exceedingly poor compressibility. This is possible if LAMCL exhibits very low plasticity, which leads to small bonding area in the tablet.

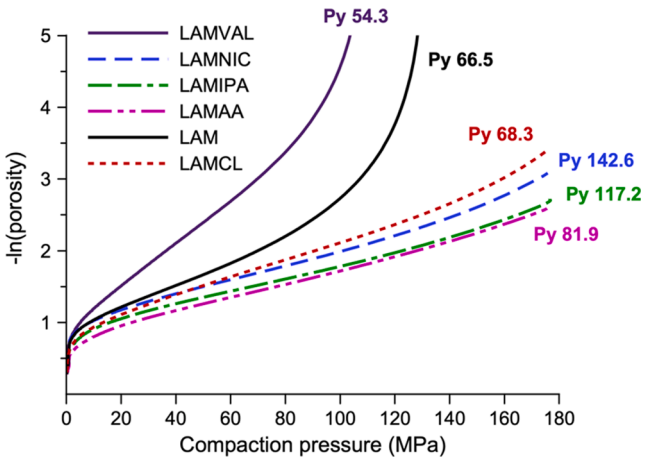

Fig. 6. In-die Heckel analysis of the six solid forms of LAM.

A powder with a lower mean yield pressure (P_y) is more plastic (Heckel, 1961; Sun and Grant, 2001c). By this measure, the plasticity of the materials follows the descending order of LAMVAL > LAM ≈ LAMCL > LAMAA > LAMIPA > LAMNIC (Fig. 6 and Table 1). This rank order differs from that based on compressibility (Fig. 5c). The discrepancy may be attributed to the complex particle deformation mechanisms during compression, including rearrangement, fragmentation, elastic, and plastic deformation (Leuenberger and Rohera, 1986). All of these mechanisms can have an influence on bonding area formed between particles in a tablet, but in-die Heckel analysis can only capture the

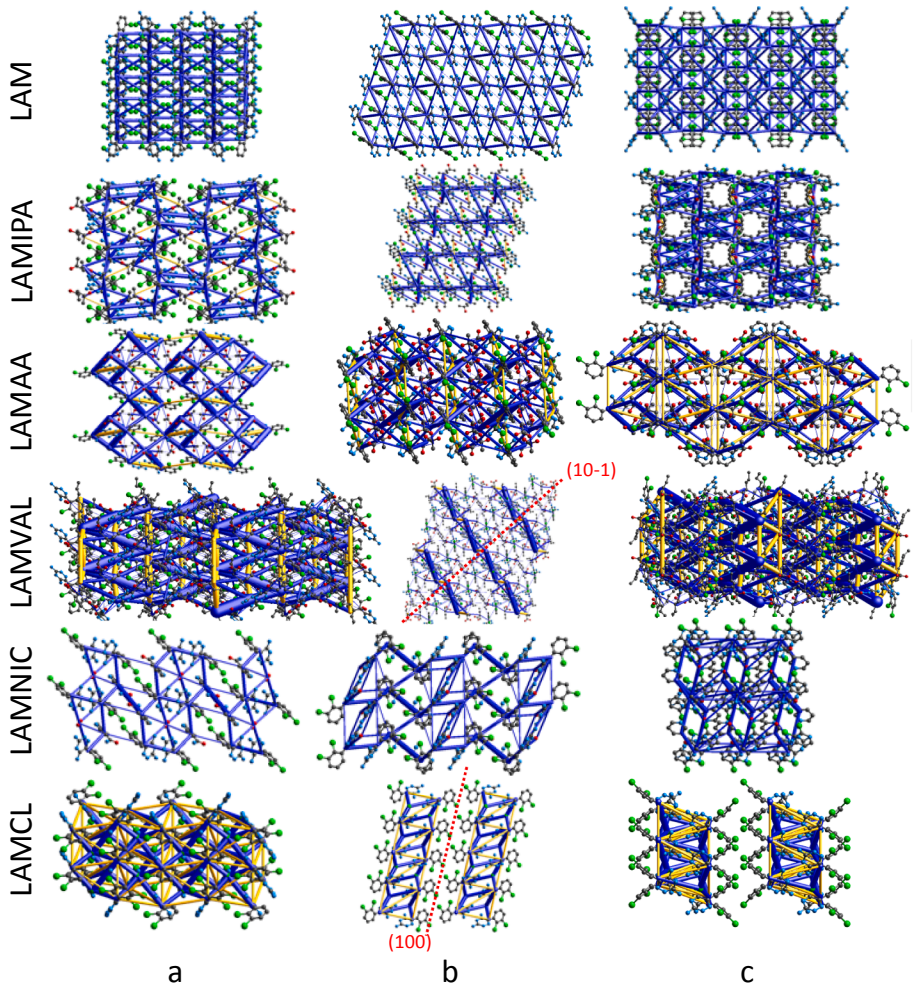

Fig. 7. Energy frameworks for lamotrigine solid forms.

Table 2
Key results from the topology analysis and morphology prediction of the six lamotrigine solid forms.

Material	Packing feature	Possible slip plane	Layer spacing (Å) *	d-spacing (Å)	Aspect ratio
LAM	3D lattice	(1 0 −1)	0.86	6.29	2.08
LAMAA	2D sheet	(1 0 −2)	−0.44	5.50	2.17
LAMCL	2D sheet	(1 0 0)	1.22	16.26	6.50
LAMVAL	2D sheet	(1 0 −1)	−2.0	21.35	3.24
LAMIPA	2D sheet	(1 0 −3)	−1.38	6.31	2.03
LAMNIC	3D lattice	(0 0 1)	0.24	14.18	2.49

* Negative value means layer interdigitated.

contributions due to plastic deformation. Thus, although the Heckel analysis remains a useful tool in studying tablet compression (Rue and Rees, 1978; Sun and Grant, 2001c), other relevant properties, such as bonding strength and particle size, must be considered along with Heckel analysis to more accurately predict tableting behaviour of powders.

Changes in crystal packing can lead to considerable changes in crystal mechanical properties (Karki et al., 2009; Mishra and Sun, 2020). For example, the different compaction properties between orthorhombic and monoclinic polymorphs of paracetamol could be explained by their different topological features of stacking molecular layers (Di Martino et al., 1996). This is one of the reasons why solid form screening is a cornerstone of research and development for new drugs (Aaltonen et al., 2009). Since the seminal work by Pertsin and Kitaigorodsky (Pertsin and Kitaigorodsky, 1987), a significant amount of work on predicting mechanical properties from crystal structures has been published (Chen et al., 2020; Roberts et al., 2000; Singaraju et al., 2020; Sun and Grant, 2001a). Although initial efforts relied on visual analysis of crystal structures, more quantitative crystal structure analysis techniques, such as energy framework and crystal structure topology analysis, have improved the ability to predict crystal mechanical properties from crystal structure (Turner et al., 2015; Wang and Sun, 2019, 2018). Within this context, energy framework (Fig. 7) and crystal structure topology analysis (Table 2) were employed to understand the powder behaviour of the various solids of LAM.

The LAM crystal has multiple intersecting planes, i.e., (2 0 0), (1 1 −1), (1 1 0), and (2 0 −2), with similar attachment energies (−102.31, −138.39, −139.4 and −145.54 kcal/mol, respectively). The topology analysis also revealed the 3D hydrogen bonding network (Table. 2). Therefore, LAM is expected to exhibit a low plasticity during compaction because of the absence of a facile slip plane from energetic perspective. However, the (1 0 −1) could serve as slip plane based on the positive layer distance. LAMIPA has intersecting planes (1 0 0), (0 0 2) and (0 1 1), covering similar facet areas (39, 18 and 37%) and with similar interaction energies (−193, −127 and −131 kcal/mol). Hence, this crystal is also not expected to exhibit appreciable plasticity. LAMNIC also has a number of intersecting planes, (10–1), (0 0 1), (0 1 0), with attachment energies of −56, −33 and −39 kcal/mol and covering facet areas of the crystal of 16, 37 and 29%, respectively. LAMAA reveals intersecting planes (1 0 0), (0 2 0) and (0 1 1) with interaction energies

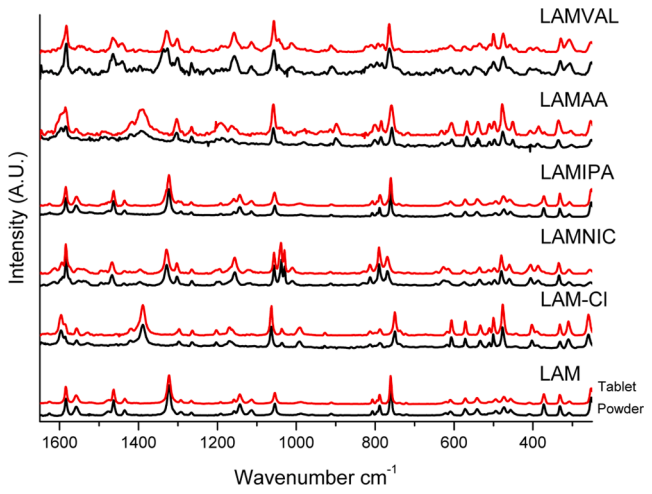

Fig. 8. Raman spectra of LAM solid forms pre- and post-compaction.

(−151, −120 and −90 kcal/mol), suggesting difficulty with plastic deformation during compression.

LAMVAL crystal shows a more anisotropic distribution of interaction energies, revealing a possible slip plane of (1 0 −1) with relatively low attachment energy of −90 kcal/mol. This makes it possible for the LAMVAL crystal to undergo plastic deformation through slip of the (1 0 −1) planes. Although all the layers are interdigitated (Table 2), the large (70%) facet area of the (1 0 −1) further magnifies the anisotropy of LAMVAL (the second highest aspect ratio among the predicted crystal morphology). Thus, compared to the previous four LAM crystal forms, the activation of slip plane (1 0 −1) leads to higher plasticity of the LAMVAL powder during compression. The energy framework confirmed that there are stacking (1 0 −1) molecular layers, with weak interlayer interaction energy, which can shear along the *b* direction.

The energy framework of LAMCL (Fig. 7) also reveals anisotropic interaction energies and a possible slip plane of (1 0 0), which has significantly lower attachment energy (−18 kJ/mol) and the largest interlayer distance (1.22 Å). The (1 0 0) facet also accounts for approximately 70% of the facet area in the calculated crystal morphology. Therefore, LAMCL is expected to exhibit better plasticity than LAMVAL. However, this is not the case as its P_y is higher than both LAM and LAMVAL (Table 1). Moreover, it exhibits the worst tabletability in this series and no intact tablets could be formed, despite better plasticity predicted from energy framework and P_y than other three LAM crystal forms. To either confirm or exclude the possibility of solid form changes induced by compaction (Chan and Doelker, 1985; Matsumoto et al., 1991; Otsuka, 1993), Raman spectroscopy was performed on powders and compressed tablets. However, no any sign of phase changes induced by compression were observed (Fig. 8).

We then investigated the elastic recovery (Table 1) and ejection forces (Fig. 9) to better understand the different tabletabilities of various LAM solid forms, as high values in these variables have been linked to the introduction of defects into tablets upon ejection (Paul and Sun, 2017b; Singaraju et al., 2020). The elastic recovery of the solid forms follows the descending order of LAMVAL > LAMCL > LAMAA > LAMNIC ≈ LAM > LAMIPA. Although LAMVAL has the highest elastic recovery, it has the best tableting properties. With the exception of LAMCL, the other forms have similar elastic recovery. In-die ejection forces (Fig. 9) descend in the order of LAM > LAMCL > LAMAA ≈ LAMIPA ≈ LAMNIC > LAMVAL. The high ejection forces of LAM and LAMCL may contribute to their poor tabletability (Fig. 5a). This is consistent with the observation that the relatively low ejection force of LAMVAL tablets corresponds to good tabletability (Fig. 5a). However, further investigation is required to explain the discrepancy between predicted and observed tabletability of LAMCL.

4. Conclusion

This work illustrates that it is possible to modulate the mechanical properties of LAM by modifying crystal structures through the formation of multi-component solids. Although LAMIPA and LAMNIC have the best powder flow properties, all the powders fail the flowability criteria for direct compression. Hence, all crystal forms will need to be formulated to ensure they have adequate flow for successful tablet manufacturing. The different flow properties could be rationalised by different crystal morphologies, but flow properties of agglomerates may still be poor due to fragmentation under stress. Among the six crystal forms, LAMVAL has the best tableting properties, which may be attributed to the presence of slip planes in its crystal structure. The observation that both LAMVAL and LAMNIC exhibit improved tableting properties than the parent drug (LAM) suggests that, when possible, the formation of multidrug crystals may be a more effective approach over simply blends of different drug crystals for direct compression. In such

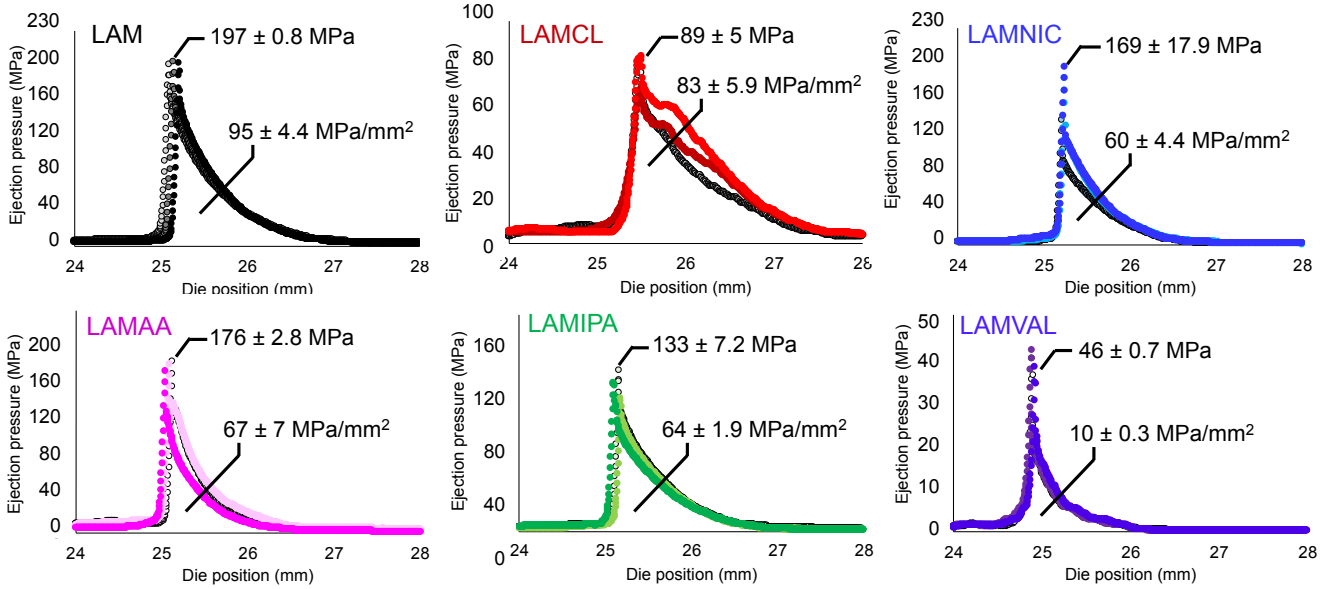

Fig. 9. Tablet ejection profiles annotated with maximum ejection pressure and area under curve of the six solid forms of LAM after compaction at 175 MPa (n = 3).

cases, less excipients are needed to attain adequate tabletability so that smaller tablets can be prepared to deliver the same amount of drug.

Credit Author Statement

O.K. was responsible for the conceptualisation, methodology, investigation, visualisation. C.W. and C.C. Sun preformed the energy framework analysis. G.W. acquired financial support to enable the work and supervised the project. All authors discussed the results and contributed to the writing, reviewing and editing of the data within the manuscript.

Declaration of Competing Interest

The authors declare the following financial interests/personal relationships which may be considered as potential competing interests: [A European (patent application no. 19166734.4, LAMVAL Co-Crystal Formulation) has been filed for LAMVAL based on the results reported previously.].

Acknowledgements

OK wishes to thank the Irish Fulbright Commission for their support to facilitate this collaboration and Fiona Hogan and Caoimhe Murphy for their help in obtaining preliminary data and for stimulating discussions. This publication was also supported by a research grant from Science Foundation Ireland (12/RC/2275/2). 12/RC/2275/2 is co-funded under the European Regional Development Fund. We acknowledge the Minnesota Supercomputing Institute (MSI) at the University of Minnesota for providing resources that contributed to the research results reported within this paper. URL: http://www.msi.umn.edu.

Appendix A. Supplementary material

Supplementary data to this article can be found online at https://doi.org/10.1016/j.ijpharm.2021.120274

References

Aaltonen, J., Allesø, M., Mirza, S., Koradia, V., Gordon, K.C., Rantanen, J., 2009. Solid form screening - A review. Eur. J. Pharm. Biopharm. https://doi.org/10.1016/j.ejpb.2008.07.014.

Ainurofiq, A., Mauludin, R., Mudhakir, D., Umeda, D., Soewandhi, S.N., Putra, O.D., Yonemochi, E., 2018. Improving mechanical properties of desloratadine via multicomponent crystal formation. Eur. J. Pharm. Sci. 111, 65–72. https://doi.org/10.1016/j.ejps.2017.09.035.

Beck, R., Nysæter, T.O., Enstad, G.G., Malthe-Sørenssen, D., Andreassen, J.-P., 2010. Influence of crystal properties on powder flow behavior of an aromatic amine and L-glutamic acid. Part. Sci. Technol. 28, 146–160. https://doi.org/10.1080/02726350903500690.

Bika, D.G., Gentzler, M., Michaels, J.N., 2001. Mechanical properties of agglomerates. Powder Technol. 117, 98–112. https://doi.org/10.1016/S0032-5910(01)00318-7.

Bolhuis, G.K., Armstrong, N.A., 2006. Excipients for direct compaction - An update. Pharm. Dev. Technol. 11, 111.

Bryant, M.J., Maloney, A.G.P., Sykes, R.A., 2018. Predicting mechanical properties of crystalline materials through topological analysis. CrystEngComm. https://doi.org/10.1039/c8ce00454d.

Chan, H.K., Doelker, E., 1985. Polymorphic transformation of some drugs under compression. Drug Dev. Ind. Pharm. 11, 315–332. https://doi.org/10.3109/03639048509056874.

Chen, H., Wang, C., Kang, H., Zhi, B., Haynes, C.L., Aburub, A., Sun, C.C., 2020. Microstructures and pharmaceutical properties of ferulic acid agglomerates prepared by different spherical crystallization methods. Int. J. Pharm. 574, 118914. https://doi.org/10.1016/j.ijpharm.2019.118914.

Cordts, E., Steckel, H., 2012. Capabilities and limitations of using powder rheology and permeability to predict dry powder inhaler performance. Eur. J. Pharm. Biopharm. 82, 417–423. https://doi.org/10.1016/j.ejpb.2012.07.018.

Council of Europe, 2019. European Pharmacopoeia. Powder flow. https://doi.org/01/2014:0906.

Dave, V.S., Saoji, S.D., Raut, N.A., Haware, R.V., 2015. Excipient variability and its impact on dosage form functionality. J. Pharm. Sci. 104, 906–915. https://doi.org/10.1002/jps.24299.

Di Martino, P., Guyot-Hermann, A.M., Conflant, P., Drache, M., Guyot, J.C., 1996. A new pure paracetamol for direct compression: The orthorhombic form. Int. J. Pharm. 128, 1–8. https://doi.org/10.1016/0378-5173(95)04127-3.

Frisch, M.J., Trucks, G.W., Schlegel, H.B., Scuseria, G.E., Robb, M.A., Cheeseman, J.R., Scalmani, G., Barone, V., Mennucci, B., Petersson, G.A., Nakatsuji, H., Caricato, M., Li, X., Hratchian, H.P., Izmaylov, A.F., Bloino, J., Zheng, G., Sonnenberg, J.L., Hada, M., Ehara, M., Toyota, K., Fukuda, R., Hasegawa, J., Ishida, M., Nakajima, T., Honda, Y., Kitao, O., Nakai, H., Vreven, T., Montgomery, J.A., Peralta, J.E., Ogliaro, F., Bearpark, M., Heyd, J.J., Brothers, E., Kudin, K.N., Staroverov, V.N., Kobayashi, R., Normand, J., Raghavachari, K., Rendell, A., Burant, J.C., Iyengar, S.S., Tomasi, J., Cossi, M., Rega, N., Millam, J.M., Klene, M., Knox, J.E., Cross, J.B., Bakken, V., Adamo, C., Jaramillo, J., Gomperts, R., Stratmann, R.E., Yazyev, O., Austin, A.J., Cammi, R., Pomelli, C., Ochterski, J.W., Martin, R.L., Morokuma, K., Zakrzewski, V. G., Voth, G.A., Salvador, P., Dannenberg, J.J., Dapprich, S., Daniels, A.D., Farkas, Foresman, J.B., Ortiz, J. V, Cioslowski, J., Fox, D.J., 2009. Gaussian 09, Revision B.01. Gaussian 09, Revis. B.01, Gaussian, Inc., Wallingford CT.

Fu, X., Huck, D., Makein, L., Armstrong, B., Willen, U., Freeman, T., 2012. Effect of particle shape and size on flow properties of lactose powders. Particuology 10, 203–208. https://doi.org/10.1016/j.partic.2011.11.003.

Han, X., Ghoroi, C., Davé, R., 2013. Dry coating of micronized API powders for improved dissolution of directly compacted tablets with high drug loading. Int. J. Pharm. 442, 74–85. https://doi.org/10.1016/j.ijpharm.2012.08.004.

Heckel, R.W., 1961a. Density-Pressure Relationships in Powder Compaction. Trans. Metall. Soc. AIME 221, 671–675.

Heckel, R.W., 1961b. An Analysis of Powder Compaction Phenomena. Trans. Metall. Soc. AIME.

Hiendrawan, S., Veriansyah, B., Widjojokusumo, E., Soewandhi, S.N., Wikarsa, S., Tjandrawinata, R.R., 2016. Physicochemical and mechanical properties of paracetamol cocrystal with 5-nitroisophthalic acid. Int. J. Pharm. 497, 106–113. https://doi.org/10.1016/j.ijpharm.2015.12.001.

Hou, H., Sun, C.C., 2008. Quantifying effects of particulate properties on powder flow properties using a ring shear tester. J. Pharm. Sci. 97, 4030–4039. https://doi.org/10.1002/jps.21288.

Joiris, E., Di Martino, P., Berneron, C., Guyot-Hermann, A.M., Guyot, J.C., 1998. Compression behavior of orthorhombic paracetamol. Pharm. Res. 15, 1122–1130. https://doi.org/10.1023/A:1011954800246.

Joshi, T.V., Singaraju, A.B., Shah, H.S., Morris, K.R., Stevens, L.L., Haware, R.V., 2018. Structure-mechanics and compressibility profile study of flufenamic acid: Nicotinamide cocrystal. Cryst. Growth Des. 18, 5853–5865. https://doi.org/10.1021/acs.cgd.8b00534.

Karki, S., Friščić, T., Fabián, L., Laity, P.R., Day, G.M., Jones, W., 2009. Improving mechanical properties of crystalline solids by cocrystal formation: new compressible forms of paracetamol. Adv. Mater. 21, 3905–3909. https://doi.org/10.1002/adma.200900533.

Kavanagh, O.N., Albadarin, A.B., Croker, D.M., Healy, A.M., Walker, G.M., 2018. Maximising success in multidrug formulation development: A review. J. Control. Release. https://doi.org/10.1016/j.jconrel.2018.05.024.

Kavanagh, O.N., Croker, D.M., Walker, G.M., Zaworotko, M.J., 2019a. Pharmaceutical cocrystals: from serendipity to design to application. Drug Discov. Today. https://doi.org/10.1016/j.drudis.2018.11.023.

Kavanagh, O.N., Walker, G., Lusi, M., 2019b. Graph-set analysis helps to understand charge transfer in a novel ionic cocrystal when the δp Ka rule fails. Cryst. Growth Des. 19, 5308–5313. https://doi.org/10.1021/acs.cgd.9b00770.

Kebler, L.F., 1914. The tablet industry – its evolution and present status – the composition of tablets and methods of analysis. J. Am. Pharm. Assoc. 3, 820–848. https://doi.org/10.1002/jps.3080030614.

Krantz, M., Zhang, H., Zhu, J., 2009. Characterization of powder flow: Static and dynamic testing. Powder Technol. 194, 239–245. https://doi.org/10.1016/j.powtec.2009.05.001.

Lee, S.L., O'Connor, T.F., Yang, X., Cruz, C.N., Chatterjee, S., Madurawe, R.D., Moore, C. M.V., Yu, L.X., Woodcock, J., 2015. Modernizing pharmaceutical manufacturing: from batch to continuous production. J. Pharm. Innov. https://doi.org/10.1007/s12247-015-9215-8.

Leuenberger, H., Rohera, B.D., 1986. Fundamentals of Powder Compression I. The Compactibility and Compressibility of Pharmaceutical Powders. Pharm. Res. An Off. J. Am. Assoc. Pharm. Sci. https://doi.org/10.1023/A:1016364613722.

Li, C.J., Trost, B.M., 2008. Green chemistry for chemical synthesis. Proc. Natl. Acad. Sci. U. S. A. https://doi.org/10.1073/pnas.0804348105.

Li, J., Abramov, Y.A., Doherty, M.F., 2017. New tricks of the trade for crystal structure refinement. ACS Cent. Sci. https://doi.org/10.1021/acscentsci.7b00130.

Mascia, S., Heider, P.L., Zhang, H., Lakerveld, R., Benyahia, B., Barton, P.I., Braatz, R.D., Cooney, C.L., Evans, J.M.B., Jamison, T.F., Jensen, K.F., Myerson, A.S., Trout, B.L., 2013. End-to-end continuous manufacturing of pharmaceuticals: Integrated synthesis, purification, and final dosage formation. Angew. Chemie - Int. Ed. 52, 12359–12363. https://doi.org/10.1002/anie.201305429.

Matsumoto, T., Kaneniwa, N., Higuchi, S., Otsuka, M., 1991. Effects of temperature and pressure during compression on polymorphic transformation and crushing strength of chlorpropamide tablets. J. Pharm. Pharmacol. 43, 74–78. https://doi.org/10.1111/j.2042-7158.1991.tb06635.x.

Mishra, M.K., Sun, C.C., 2020. Conformation directed interaction anisotropy leading to distinct bending behaviors of Two ROY polymorphs. Cryst. Growth Des. https://doi.org/10.1021/acs.cgd.0c00521.

Osei-Yeboah, F., Chang, S.Y., Sun, C.C., 2016. A critical examination of the phenomenon of bonding area - Bonding strength interplay in powder tableting. Pharm. Res. https://doi.org/10.1007/s11095-016-1858-8.

Otsuka, M., 1993. Effects of environmental temperature and compression energy on polymorphic transformation during tabletting. Drug Dev. Ind. Pharm. 19, 2241–2269. https://doi.org/10.3109/03639049309047191.
Paul, S., Sun, C.C., 2017a. The suitability of common compressibility equations for characterizing plasticity of diverse powders. Int. J. Pharm. https://doi.org/10.1016/j.ijpharm.2017.08.096.
Paul, S., Sun, C.C., 2017b. Gaining insight into tablet capping tendency from compaction simulation. Int. J. Pharm. https://doi.org/10.1016/j.ijpharm.2017.03.073.
Pertsin, A.J., Kitaigorodsky, A.I., 1987. The Atom-Atom Potential Method. Springer, Berlin, Heidelberg, pp. 69–148. https://doi.org/10.1007/978-3-642-82712-9_3.
Podczeck, F., 2013. "methods for the practical determination of the mechanical strength of tablets - From empiricism to science" (Podczeck, 2012): Response to Jørn Sonnergaard's comments (2013). Int. J. Pharm. https://doi.org/10.1016/j.ijpharm.2013.01.066.
Podczeck, F., 2012. Methods for the practical determination of the mechanical strength of tablets - From empiricism to science. Int. J. Pharm. https://doi.org/10.1016/j.ijpharm.2012.06.059.
Poechlauer, P., Manley, J., Broxterman, R., Gregertsen, B., Ridemark, M., 2012. Continuous processing in the manufacture of active pharmaceutical ingredients and finished dosage forms: An industry perspective. Org. Process Res. Dev. 16, 1586–1590. https://doi.org/10.1021/op300159y.
Prescott, J.K., Barnum, R.A., 2000. On powder flowability. Pharm. Technol. 60–84.
Ridgway, K., Rupp, R., 1969. The effect of particle shape on powder properties. J. Pharm. Pharmacol. 21, 30S–39S. https://doi.org/10.1111/j.2042-7158.1969.tb08344.x.
Roberts, R.J., Payne, R.S., Rowe, R.C., 2000. Mechanical property predictions for polymorphs of sulphathiazole and carbamazepine. Eur. J. Pharm. Sci. 9, 277–283. https://doi.org/10.1016/S0928-0987(99)00065-2.
Rue, P.J., Rees, J.E., 1978. Limitations of the Heckel relation for predicting powder compaction mechanisms. J. Pharm. Pharmacol. 30, 642–643. https://doi.org/10.1111/j.2042-7158.1978.tb13347.x.
Sanphui, P., Mishra, M.K., Ramamurty, U., Desiraju, G.R., 2015. Tuning mechanical properties of pharmaceutical crystals with multicomponent crystals: Voriconazole as a case study. Mol. Pharm. 12, 889–897. https://doi.org/10.1021/mp500719t.
Schaller, B.E., Moroney, K.M., Castro-Dominguez, B., Cronin, P., Belen-Girona, J., Ruane, P., Croker, D.M., Walker, G.M., 2019. Systematic development of a high dosage formulation to enable direct compression of a poorly flowing API: A case study. Int. J. Pharm. 566, 615–630. https://doi.org/10.1016/j.ijpharm.2019.05.073.
Shekunov, B.Y., Chattopadhyay, P., Tong, H.H.Y., Chow, A.H.L., 2007. Particle size analysis in pharmaceutics: Principles, methods and applications. Pharm. Res. https://doi.org/10.1007/s11095-006-9146-7.
Singaraju, A.B., Bahl, D., Wang, C., Swenson, D.C., Sun, C.C., Stevens, L.L., 2020. Molecular Interpretation of the Compaction Performance and Mechanical Properties of Caffeine Cocrystals: A Polymorphic Study. Mol. Pharm. 17, 21–31. https://doi.org/10.1021/acs.molpharmaceut.9b00377.
Sonnergaard, J., 2013. From empiricism to science? Int. J. Pharm. https://doi.org/10.1016/j.ijpharm.2013.01.033.
Strickland, W.A., Nelson, E., Busse, L.W., Higuchi, T., 1956. The physics of tablet compression. IX. Fundamental aspects of tablet lubrication. J. Am. Pharm. Assoc. Am. Pharm. Assoc. (Baltim) 45, 51–55. https://doi.org/10.1002/jps.3030450116.
Suihko, E., Lehto, V.P., Ketolainen, J., Laine, E., Paronen, P., 2001. Dynamic solid-state and tableting properties of four theophylline forms. Int. J. Pharm. 217, 225–236. https://doi.org/10.1016/S0378-5173(01)00607-X.
Sun, C.C., Grant, D.J.W., 2001a. Influence of crystal structure on the tableting properties of sulfamerazine polymorphs. Pharm. Res. 18, 274–280. https://doi.org/10.1023/A:1011038526805.
Sun, C.C., Grant, D.J.W., 2001b. Influence of crystal shape on the tableting performance of L-lysine monohydrochloride dihydrate. J. Pharm. Sci. 90, 569–579. https://doi.org/10.1002/1520-6017(200105)90:5<569::AID-JPS1013>3.0.CO;2-4.
Sun, C.C., Grant, D.J.W., 2001c. Influence of elastic deformation of particles on Heckel analysis. Pharm. Dev. Technol. 6, 193–200. https://doi.org/10.1081/PDT-100000738.
Tran, D.T., Majerová, D., Veselý, M., Kulaviak, L., Ruzicka, M.C., Zámostný, P., 2019. On the mechanism of colloidal silica action to improve flow properties of pharmaceutical excipients. Int. J. Pharm. 556, 383–394. https://doi.org/10.1016/j.ijpharm.2018.11.066.
Turner, M.J., Grabowsky, S., Jayatilaka, D., Spackman, M.A., 2014. Accurate and efficient model energies for exploring intermolecular interactions in molecular crystals. J. Phys. Chem. Lett. https://doi.org/10.1021/jz502271c.
Turner, M.J., McKinnon, J.J., Wolff, S.K., Grimwood, D.J., Spackman, P.R., Jayatilaka, D., Spackman, M.A., 2017. CrystalExplorer (Version 17.5). Univ. West. Aust. Perth.
Turner, M.J., Thomas, S.P., Shi, M.W., Jayatilaka, D., Spackman, M.A., 2015. Energy frameworks: Insights into interaction anisotropy and the mechanical properties of molecular crystals. Chem. Commun. https://doi.org/10.1039/c4cc09074h.
Wang, C., Paul, S., Wang, K., Hu, S., Sun, C.C., 2017. Relationships among Crystal Structures, Mechanical Properties, and Tableting Performance Probed Using Four Salts of Diphenhydramine. Cryst. Growth Des. 17, 6030–6040. https://doi.org/10.1021/acs.cgd.7b01153.
Wang, C., Sun, C.C., 2019. Computational techniques for predicting mechanical properties of organic crystals: A systematic evaluation. Mol. Pharm. https://doi.org/10.1021/acs.molpharmaceut.9b00082.
Wang, C., Sun, C.C., 2018. Identifying slip planes in organic polymorphs by combined energy framework calculations and topology analysis. Cryst. Growth Des. https://doi.org/10.1021/acs.cgd.8b00202.
Yadav, J.P., Yadav, R.N., Uniyal, P., Chen, H., Wang, C., Sun, C.C., Kumar, N., Bansal, A.K., Jain, S., 2020. Molecular interpretation of mechanical behavior in four basic crystal packing of isoniazid with homologous cocrystal formers. Cryst. Growth Des. https://doi.org/10.1021/acs.cgd.9b01224.
York, P., 1975. Application of powder failure testing equipment in assessing effect of glidants on flowability of cohesive pharmaceutical powders. J. Pharm. Sci. 64, 1216–1221. https://doi.org/10.1002/jps.2600640721.
Zhou, Q., Shi, L., Marinaro, W., Lu, Q., Sun, C.C., 2013. Improving manufacturability of an ibuprofen powder blend by surface coating with silica nanoparticles. Powder Technol. https://doi.org/10.1016/j.powtec.2013.08.031.